Neural Modeling of High-Frequency Forward Transmission Coefficient for HEMT and FinFET Technologies

Zlatica Marinković[1], Giovanni Crupi[2], Dominique M. M.-P. Schreurs[3], Alina Caddemi[2], and Vera Marković[1]

Abstract – **This paper is devoted to examining the ability of artificial neural networks to model the forward transmission coefficient, which represents an important figure of merit for microwave transistors. This analysis is carried out for two different on-wafer devices, namely GaAs HEMT and Si FinFET. As far as the HEMT technology is concerned, the model is developed for three devices which differ in gate width. For the FinFET technology, the model is determined not only for the whole device but also for the actual transistor by using the de-embedding procedure to subtract the effects of pads, transmission lines, and substrate from the measurements. The obtained models have been developed and validated in a wide range of bias conditions for a frequency range up to 50 GHz.**

Keywords – **Artificial Neural Networks, FinFET, Forward Transmission Coefficient, HEMT, microwave frequency**

I. Introduction

In the past two decades artificial neural networks (ANNs) have been applied in lots of applications for modeling microwave devices and circuits [1]-[13]. They are suitable for modeling applications because of their capabilities to learn and to generalize. As a matter of fact, ANNs learn relationships between two sets of data and, once properly developed, give correct response even for input values not included in the set used for the ANN learning. Among the ANN applications in the microwave field, there are applications addressed to model microwave transistors. ANNs have been applied for representing DC, small-signal (including noise), and large-signal behaviour of microwave transistors [3]-[13].

In the present paper, the attention is focused on neural modeling of the forward transmission coefficient S_{21}. This study is carried out on two different advanced microwave FET technologies, namely high electron-mobility transistors (HEMTs) [14]-[18] and fin field-effect transistors (FinFETs) [19]-[20]. In earlier work we have shown that ANNs can be successfully applied for building a multi-bias small-signal model for both types of devices [11]-[13]. The aim of this paper is to provide a more detailed analysis of the modeling for the forward transmission coefficient. This scattering parameter has been chosen to be investigated here due to its importance as figure of merit for the transistor gain. Furthermore, its modeling is quite challenging because the dynamic of its variations as the operating bias point changes is the highest compared to the other three scattering parameters.

For the HEMT technology we have analysed three devices with different gate width, whereas for FinFETs the analysis has been done for the whole device as well as for the actual transistor, which is obtained after removing the effects of pads, transmission lines, and substrate.

The paper is organized as follows. A brief description of the theoretical background on the ANN modeling technique is given in Section II. In Section III the modeling of HEMT devices is described, and subsequently, in Section IV the obtained results are presented. Section V describes the details of the modeling technique for FinFETs. Analyses and validation of the developed models for both whole and actual devices are given in Section VI. The achieved concluding remarks are given in Section VII.

II. ANN Modeling Technique

For both technologies, the modeling of the forward transmission coefficient is based on multi-layer perceptron (MLP) ANNs [2]. An MLP ANN consists of layers of neurons: an input layer, an output layer, and one or more hidden layers. The number of neurons in the input layer equals the number of independent input parameters, whereas the number of the output neurons equals the number of parameters to be modeled by the ANN. An ANN is trained to learn dependencies between two data sets by optimization of thresholds of the neuron activation functions and the neuron connection weights. One of the most frequently used optimization algorithms is the so-called backpropagation algorithm and its modifications with a higher order of convergence, namely the quasi-Newton and Levenberg-Marquardt algorithms [2].

Once ANNs have been trained properly, the outputs can be determined directly from the ANNs, by finding the response of the ANNs for the given input values.

In the case of the forward transmission coefficient modeling the ANN outputs correspond to the real and

[1] Z. Marinković and V. Marković are with the University of Niš, Faculty of Electronic Engineering, Aleksandra Medvedeva 14, 18000 Niš, Serbia, E-mail: zlatica.marinkovic@elfak.ni.ac.rs, vera.markovic@elfak.ni.ac.rs

[2] G. Crupi and A. Caddemi are with the University of Messina, Dipartimento di Fisica della Materia e Ingegneria Elettronica, 98166 Messina, Italy, E-mail: giocrupi@ingegneria.unime.it, caddemi@ingegneria.unime.it

[3] D. M. M.-P. Schreurs is with the Katholieke Universiteit Leuven, Electronic Engineering Department, B-3001 Leuven, Belgium, E-mail: dominique.schreurs@esat.kuleuven.be

imaginary parts of S_{21}. Therefore, the forward transmission coefficient can be modeled by one two-output ANN having at the outputs the real and imaginary parts. Nevertheless, to ensure accurate modeling the considered basic ANN model consists of two one-output ANNs trained to reproduce separately real and imaginary parts of the coefficient, as will be illustrated in details in the following sections.

The measured forward transmission coefficient data have been used for the ANN training. Since the number of ANN hidden neurons can not be a priori known, it has been determined during the training. Namely, for each of the chosen input-output structure, ANNs with different number of hidden neurons have been trained and validated. The ANN showing the best test statistics has been chosen as the final model for the considered case.

In this paper we are using the following notation: $N-H_1-H_2-M$ represents the ANN with N neurons in the input layer, M neurons in the output layer, and H_1 and H_2 neurons in the first and second hidden layer, respectively.

To evaluate the model accuracy, the percentage errors E_{21} between measured and simulated S_{21} were calculated at each bias point as follows

$$E_{21} = \frac{1}{N_f} \sum_{N_f} 100 \left| \frac{S_{21MEASURED}(f) - S_{21SIMULATED}(f)}{S_{21MEASURED}(f)} \right| \quad (1)$$

where N_f represents the number of frequency points.

III. HEMT Neural Models

As far as the small-signal model for HEMTs is concerned, the model inputs are: input and output bias voltages, frequency, and gate width [11]. Therefore, there are four neurons in the input layer corresponding to the mentioned four input parameters. There are two ANNs in the model aimed to model the real and imaginary parts of S_{21}, as shown in Fig. 1. Each ANN is trained separately.

Fig. 1. Small-signal bias-dependent neural model for the forward transmission coefficient of HEMTs with different gate width.

IV. HEMT Modeling Results

The described modeling approach was applied to on-wafer AlGaAs/GaAs HEMTs with different gate widths: 100, 200, and 300 μm. The models were developed from the measured S-parameters. For each device the measurements were done in 101 points over the frequency range extending from 0.5 up to 50 GHz and at 546 different bias points (i.e., -1.5 V ≤ V_{gs} ≤ 0 V with 75 mV step and 0 V ≤ V_{ds} ≤ 2.5 V with 100 mV step).

Two subsets of the measured data set were used for the neural model development. The data set used for the training of the ANNs corresponds to 42 bias points (i.e., V_{gs} = {-1.35 V, -1.05 V, -0.75 V, -0.45 V, -0.15 V, 0 V} and V_{ds} = {0 V, 0.2 V, 0.8 V, 1.2 V, 1.8 V, 2.1 V, 2.5 V}). The other dataset (the test set) was used for the model generalization test and it corresponds to 34 bias points (i.e., V_{gs} = {-1.5 V, -1.2 V, -0.9 V, -0.6 V, -0.3 V, 0 V} and V_{ds} = {0 V, 0.5 V, 1 V, 1.5 V, 2 V, 2.5 V}, with excluded data corresponding to bias points included in the training set: V_{gs} = 0 V with V_{ds} = 0 V and 2.5 V, V_{gs} = -1.5 V with V_{ds} = 0 V and 2.5 V.

Among the trained ANNs with different numbers of hidden neurons, the ANNs exhibiting the best modeling accuracy were chosen for the final model. It was found that the ANNs chosen to model the real and imaginary parts of the transmission coefficient have both two hidden layers with 25 neurons in each layer (i.e., have structure 4-25-25-1).

According to the test statistics it was found that the model exhibits a very high modeling accuracy over the considered bias range. As illustration, Fig. 2 shows the comparison between measured and simulated S_{21} for a typical bias point (i.e., $V_{gs} = -0.6$ V and $V_{ds} = 2.5$ V). In Fig. 2 there are also the percentage errors calculated at the considered bias point for each of the three HEMT devices. It can be observed that good agreement between the simulated and measured data was achieved. It should be noted that the considered bias point was not included in the training of the neural model, which indicates that the neural model shows a good generalization.

It has been found that the higher percentage errors were exhibited at bias points where the S_{21} has very small values, namely "pinch-off" and/or low V_{ds} [11]. At such bias points, although the deviations of the simulations from the measured data at the "pinch-off" bias point are small in absolute amount comparing to the typical values of S_{21}, the relative percentage errors are high because the parameter values are small at "pinch-off" [12].

Complete test statistics of this model as well as comparison with the analytical multi-bias modeling approach can be found in [11]. There also information about the modeling of the three other scattering parameters can be found.

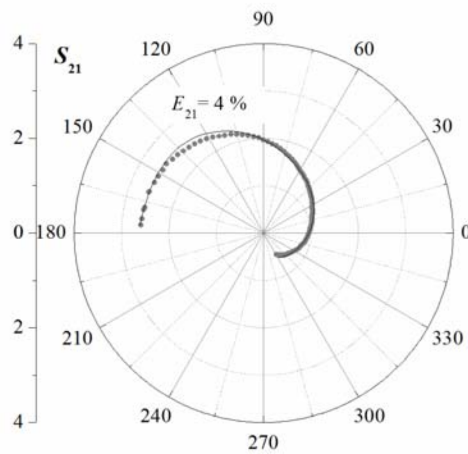

(a)

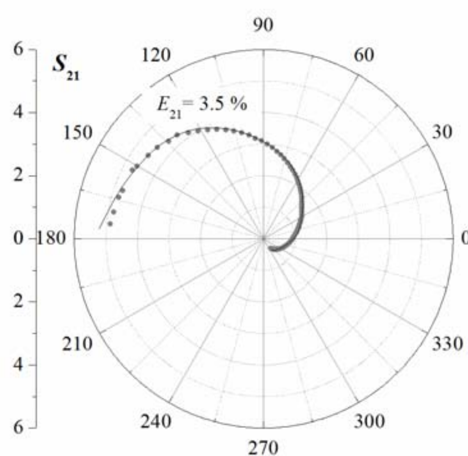

(b)

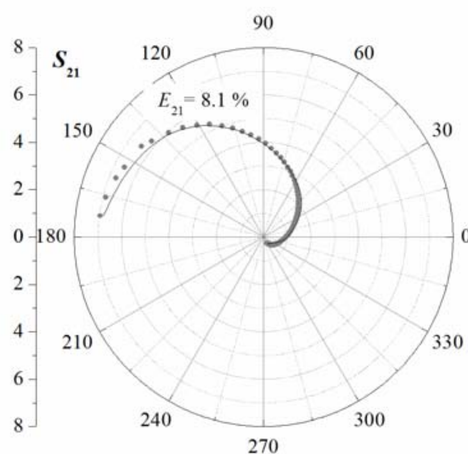

(c)

Fig. 2. Simulated (lines) and measured (symbols) S_{21} at a typical bias point (i.e., V_{gs} = -0.6 V and V_{ds} = 2.5 V) in the frequency range from 0.5 GHz to 50 GHz for three scaled HEMT devices with different gate widths: (a) 100 μm, (b) 200 μm, and (b) 300 μm.

V. FinFET Neural Models

The model presented in this work refers to a FinFET device fabricated with IMEC technology [21]. The studied multi-finger and multi-fin device has a gate length of 60 nm, a fin height of 60 nm, a fin width of 32 nm, and an amount of fingers of 30, where each finger is composed of 6 fins. The total FinFET gate width is straightforwardly proportional to the number of fins N_{fin} and number of fingers N_{finger} :

$$W = N_{fin} \cdot N_{finger}(2 H_{fin} + W_{fin}) \qquad (2)$$

where H_{fin} and W_{fin} are height and width of a fin, as shown in Fig. 3. In the case of the tested device, the total gate width is 27.36 μm.

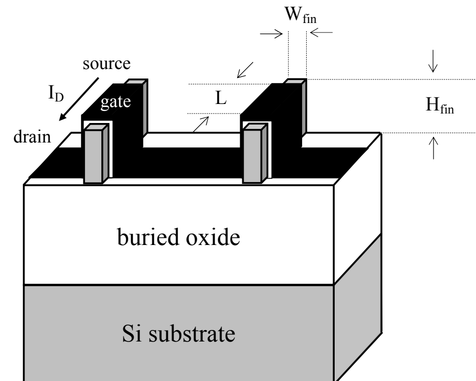

Fig. 3. Cross-section of a triple gate FinFET. Illustrative example with two fins.

As mentioned earlier, to ensure accurate modeling the considered basic ANN model consists of two one-output ANNs trained to reproduce separately real and imaginary parts of the coefficient, as shown in Fig. 4. Since the modeled real and imaginary parts are functions of the frequency and the applied bias voltages, both ANNs have three inputs. The training targets for the outputs of both ANNs are the corresponding measured values in the case of whole device. The training data in the case of actual transistor are obtained by removing the parasitic effects of pads, transmission lines, and substrate with an “open” and “short” de-embedding procedure [22]-[23].

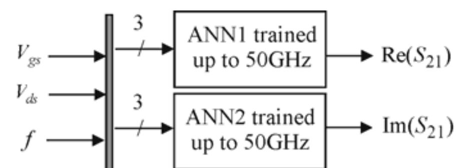

Fig. 4. Basic small-signal bias-dependent neural model for FinFET forward transmission coefficient.

The mentioned basic model is suitable for modeling the actual device. However, in case of whole device, although the basic model exhibits good accuracy averaged over the bias and frequency range, there are significant deviations of the simulated values from the target measured values in the lower part of the frequency range, namely for frequencies where the kink caused by the lossy silicon substrate appears. A deeper

analysis of the measured data shows that the kink effect has a stronger impact on the real part rather than the imaginary part of an S-parameter, as will be illustrated in the next section. Therefore, for modeling accurately the whole device over the full frequency range, we use a special structure of the model as depicted in Fig. 5.

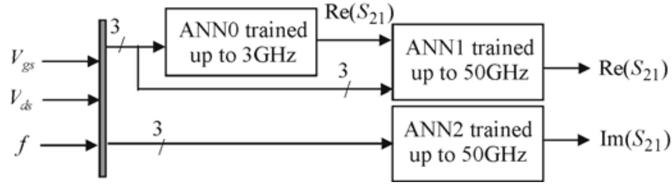

Fig. 5. Small-signal bias-dependent hierarchical PKI neural model for the whole device.

The proposed model is a two-step hierarchical neural model exploiting the so-called prior knowledge input (PKI) neural approach for modeling the real part of the transmission coefficient. The PKI ANN approach is based on introducing additional inputs to the ANN which are aimed to provide additional information about the parameters being modeled and helping in that way the ANN to find the proper relationship between sets of input and output parameters [1]-[2]. In the case of modeling the real part of a parameter, the additional prior knowledge corresponds to the real part of the considered parameter obtained from the model developed for the lower frequencies (ANN0 shown in Fig. 5). The low-frequency range is determined by the presence of the kink effect. In the studied case, the kink effect occurs at frequencies lower than 3 GHz.

Therefore, before the training process of ANN1, which gives the final value of the real part for the whole frequency range, it is necessary to develop the bias and frequency dependent neural model for the lower part of the considered frequency range.

VI. FinFET Modeling Results

The forward transmission coefficient of the investigated FinFET was measured in 201 points from 0.3 GHz to 50 GHz under 325 different bias conditions (i.e., 0 V ≤ V_{gs} ≤ 1.2 V with 50 mV step and 0 V ≤ V_{ds} ≤ 1.2 V with 100 mV step). For the training purpose, the data referring to 91 bias points uniformly distributed over the range of bias voltages were used (i.e., V_{gs} from 0 V to 1.2 V with 100 mV step and V_{ds} from 0 V to 1.2 V with 200 mV step). On the other hand, all the available data were used for evaluating the models. It is important to note that in this work uniform sampling of the training data has been applied, without doing experiment design for optimizing the number of measurements needed for the model development.

The percentage errors have been calculated for each of the 325 available bias points. Moreover, the average and maximum E_{21} values are calculated:

$$E_{21\text{avg}} = \frac{1}{N_b}\sum E_{21} \quad (3)$$

$$E_{21\max} = \max_{N_b} E_{21} \quad (4)$$

where N_b represents the number of considered bias points.

First, the basic model depicted in Fig. 4 has been developed for the whole and the actual devices. Then two-step model exploiting two ANNs for modeling the real part of the forward transmission coefficient has been developed for the whole device. Table I reports details about the ANNs chosen for the final model on the basis of the best achieved modeling accuracy.

TABLE I
Structure of ANNs Chosen for the Final Model

	Whole device (One ANN for real part)	Whole device (Two ANNs for real part)	Actual device
ANN0	-	4-25-25-1	-
ANN1	3-25-25-1	4-25-24-1	3-27-23-1
ANN2	3-24-22-1		3-26-25-1

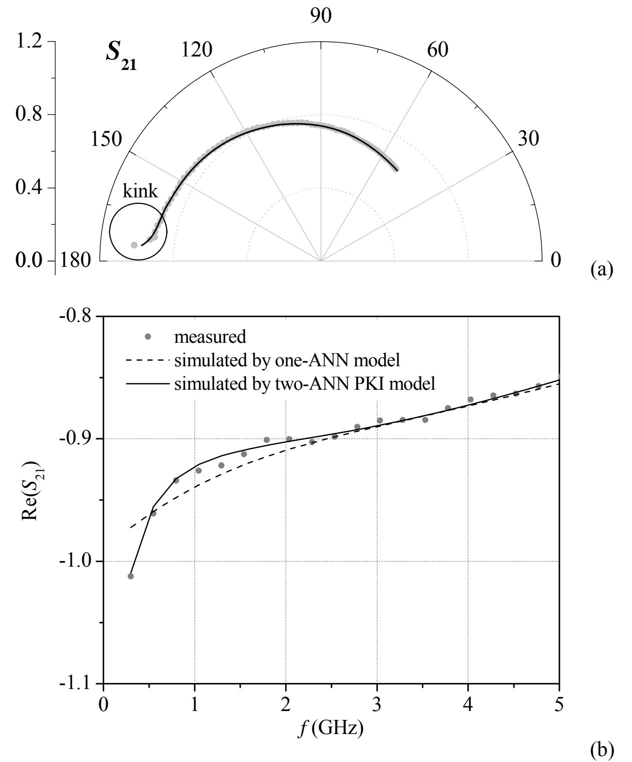

Fig. 6. Frequency dependence of S_{21} for a FinFET at V_{gs} = 0.8 V and V_{ds} = 0.8 V: (a) basic model; (b) real part at lower frequencies: measurements (symbols) and simulations (lines).

When the basic model is applied for the modeling of the whole device, the percentage error averaged over the bias range is $E_{21\text{avg}} = 1.6\,\%$ and the maximum value of the error is $E_{21\max} = 5.1\,\%$. Although these values indicate that very good modeling over the considered bias range has been achieved, detailed analysis of the error coefficient frequency dependences per each bias point has shown that the model has

not reproduced well the transmission coefficient behaviour at low frequencies where the kink effect occurs, as illustrated in Fig. 6a. As mentioned before, this has been caused by the fact that the real part of the coefficient has not been modeled properly in the lower frequency range (see Fig. 6b).

The two-ANN PKI model for the real part reproduces the real part of the transmission coefficient much better than the basic model (see Fig.6b), which has led to better reproduction of the transmission coefficient in the lower frequency range, as illustrated in Fig. 7.

From this point on, all presented results for the whole device refer to the two-step PKI ANN model.

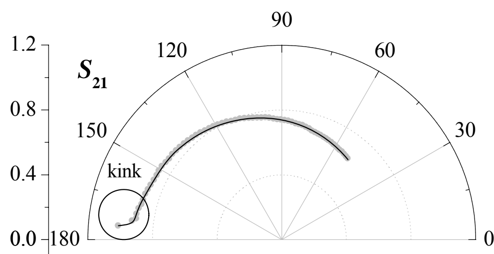

Fig. 7. Frequency dependence of S_{21} for a FinFET at V_{gs} = 0.8 V and V_{ds} = 0.8 V: measurements (symbols) and simulations obtained by two-step PKI ANN model (lines).

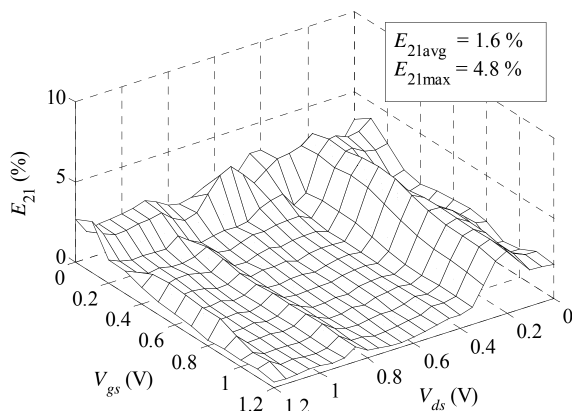

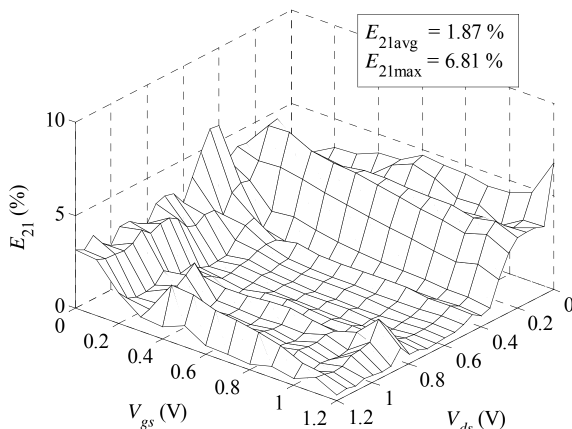

Fig. 8. Bias dependence of the percentage errors: (a) whole device; (b) actual device after applying the "open" and "short" de-embedding procedure.

Bias dependence of the percentage errors for both, whole and actual device are plotted in Fig. 8. The analysis of the obtained percentage errors shows that in both cases the average error does not exceed 2%. The maximum error is below 5% for the whole device, whereas for the actual transistor the percentage errors are higher than 5% only for 6 bias points. It should be outlined that the modeling technique exhibits very good generalization, as confirmed by the fact that 72% of the tested bias points were not used for the training of ANNs. As additional illustration of the generalization capability, Fig. 9 illustrates the prediction of the transmission coefficient for a bias point not used in the training of the ANNs for the whole and actual device. The corresponding percentage errors are shown together with the plots. Information about modeling of the other three scattering parameters can be found in [13].

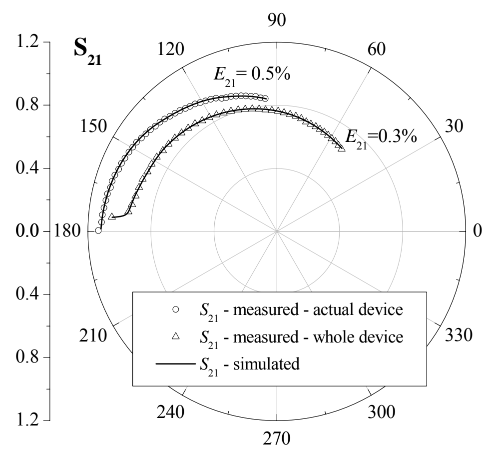

Fig. 9. S_{21} for the whole and actual device at bias point V_{gs} = 0.75 V and V_{ds} = 0.9 V which has not been used for the model development.

VII. CONCLUSION

In this paper the results of applying the ANN approach for building a multi-bias small-signal model for the transmission coefficient of microwave FETs are presented. The ANN modeling approach has been applied to three scaled HEMT devices in GaAs technology and to a Si FinFET, which has been investigated before and after applying a de-embedding procedure for removing part of the extrinsic contributions from the measurements. For both technologies, the model has been validated up to 50 GHz.

The basic model consists of two ANNs, which are aimed to model the real and imaginary parts of the transmission coefficient. Such a model has provided very good results for the HEMT devices and for the actual transistor in the case of FinFET technology. The whole FinFET device exhibits the kink effect in the lower part of the frequency range which can not be properly modeled by the basic model. Therefore, to improve the modeling for the whole device, the real part has been modeled by two-step ANN model.

The presented models exhibit very good modeling accuracy

not only for the bias points used for the model development but also for bias points not seen by the ANNs during the training. This enables accurate simulation of the considered parameter with an arbitrary grid of bias conditions.

ACKNOWLEDGEMENT

The authors thank IMEC for supplying FinFET devices. The work was supported by the project TR-32052 of the Serbian Ministry of Education and Science, by the KU Leuven GOA project and by FWO-Vlaanderen.

This paper is an extended version of the paper "*Artificial neural network based modeling of FinFET forward transmission coefficient*" presented at the 10th International Conference on Telecommunications in Modern Broadcasting, Cable and Satellite Communications – TELSIKS 2011, Niš, Serbia.

REFERENCES

[1] P. M. Watson, K. C. Gupta, and R. L. Mahajan, "Applications of knowledge-based artificial neural network modeling to microwave components," *Int. J. RF Microw. Computer-Aided Eng.*, vol. 9, no. 3, pp. 254–260, May 1999.

[2] Q. J. Zhang and K. C. Gupta, *Neural Networks for RF and Microwave Design*. Boston, MA: Artech House, 2000.

[3] F. Giannini, G. Leuzzi, G. Orengo, and M. Albertini, "Small-signal and large-signal modeling of active devices using CAD-optimized neural networks," *Int. J. RF Microw. Computer-Aided Eng.,* vol. 12, no. 1, pp. 71-78, Jan 2002.

[4] D. Schreurs, J. Verspecht, E. Vandamme, N. Vellas, C. Gaquiere, M. Germain, *et al*., "ANN Model for AlGaN/GaN HEMTs Constructed from Near-Optimal-Load Large-Signal Measurements," *IEEE Int. Microw. Symp.*, Philadelphia, PA, USA, Jun. 2003, pp. 447-450.

[5] Q. J. Zhang, K. C. Gupta, and V. K. Devabhaktuni, "Artificial neural networks for RF and microwave design—From theory to practice," *IEEE Trans. Microw. Theory Tech.*, vol. 51, no. 4, pp. 1339–1350, Apr. 2003.

[6] J. E. Rayas-Sanchez, "EM-based optimization of microwave circuits using artificial neural networks: The state-of-the-art," *IEEE Trans. Microw. Theory Tech.*, vol. 52, no. 1, pp. 420–435, Jan. 2004.

[7] H. Taher, D. Schreurs, and B. Nauwelaers, "Constitutive relations for nonlinear modeling of Si/SiGe HBTs using an ANN model," *Int. J. RF Microw. Computer-Aided Eng.*, vol. 15, no. 2, pp. 203-209, March 2005.

[8] Z. Marinković and V. Marković, "Temperature dependent models of low-noise microwave transistors based on neural networks," *Int. J. RF Microw. Computer-Aided Eng.*, vol. 15, no. 6, pp. 567-577, Nov. 2005.

[9] A. Caddemi, F. Catalfamo, and N. Donato, "A neural network approach for compact cryogenic modeling of HEMT's," *Int. J. Electron.*, vol. 94, no. 9, pp.877-887, Sept. 2007.

[10] H. Kabir, L. Zhang, M. Yu, P. Aaen, J. Wood, and Q. J. Zhang "Smart modeling of microwave devices," *IEEE Microw. Mag.*, vol. 11, pp. 105–108, May 2010.

[11] Z. Marinković, G. Crupi, A. Caddemi, and V. Marković, "Comparison between analytical and neural approaches for multibias small signal modeling of microwave scaled FETs," *Microw. Opt. Techn. Lett.*, vol. 52, no. 10, pp. 2238-2244, Oct. 2010.

[12] Z. Marinković, G. Crupi, A. Caddemi, and V. Marković, "On the neural approach for FET small-signal modeling up to 50GHz", *in Proc. 10th Seminar of Neural Network Application in Electronical Engineering - NEUREL 2010*, Belgrade, Serbia, Sept. 2010, pp. 89-92.

[13] Z. Marinković, G. Crupi, D. M. M.-P. Schreurs, A. Caddemi, and V. Marković, "Microwave FinFET modeling based on artificial neural networks including lossy silicon substrate," *Microelectron. Eng.,* vol. 88, no. 10, pp. 3158-3163, Oct. 2011.

[14] M. Berroth and R. Bosch, "Broad-band determination of the FET small-signal equivalent circuit", *IEEE Trans. Microw. Theory Tech*, vol. 38, no. 7, pp. 891-895, Jul. 1990.

[15] R. G. Brady, C. H. Oxley, and T. J. Brazil, "An improved small-signal parameter-extraction algorithm for GaN HEMT devices," *IEEE Trans. Microw. Theory Tech.*, vol. 56, no. 7, pp. 1535-1544, Jul. 2008.

[16] A. Zarate-de Landa, J. E. Zuniga-Juarez, J. R. Loo-Yau, J. A. Reynoso-Hernandez, M. C. Maya-Sanchez, and J. L. del Valle-Padilla, "Advances in linear modeling of microwave transistors," *IEEE Microw. Mag.*, vol. 10, no, 2, pp. 100, 102-111, 146, Apr. 2009.

[17] G. Crupi, D. M. M.-P. Schreurs, A. Raffo, A. Caddemi, and G. Vannini, "A new millimeter wave small-signal modeling approach for pHEMTs accounting for the output conductance time delay", *IEEE Trans. Microw. Theory Tech.*, vol. 56, no. 4, pp. 741-746, Apr. 2008.

[18] A. Caddemi, G. Crupi, and A. Macchiarella, "On-wafer scaled GaAs HEMTs: direct and robust small-signal modeling up to 50 GHz", *Microw. Opt. Techn. Lett.,* vol. 51, no. 8, pp. 1958-1963, May 2009.

[19] D. Hisamoto, W. C. Lee, J. Kedzierski, E. Anderson, H. Takeuchi, K. Asano, *et al.*, "A folded-channel MOSFET for deep-sub-tenth micron era," *in Proc. Int. Electron Devices Meeting (IEDM) Tech. Digest*, San Francisco, CA, USA, Dec. 1998, pp. 1032-1034.

[20] J.P. Colinge, "Multi-gate SOI MOSFETs", *Microelectron. Eng.*, vol. 84, no. 9/10, pp. 2071–2076, Sept./Oct. 2007.

[21] G. Crupi, D. M. M.-P. Schreurs, B. Parvais, A. Caddemi, A. Mercha, and S. Decoutere, "Scalable and multibias high frequency modeling of multi fin FETs," *Solid-State Electron.*, vol. 50, no. 10/11, pp. 1780-1786, Nov./Dec. 2006.

[22] G. Crupi, D.M.M.-P. Schreurs, A. Caddemi, "On the small signal modeling of advanced microwave FETs: a comparative study", *Int. J. RF Microw. Computer-Aided Eng.*, vol. 18, no. 5, pp. 417–425, May 2008.

[23] G. Crupi, D. M. M.-P. Schreurs, and A. Caddemi, "Accurate silicon dummy structure model for nonlinear microwave FinFET modeling," *Microelectron. J.*, vol. 41, no 9, pp. 574-578, Sept. 2010.

[24] Z. Marinković, G. Crupi, D. M. M.-P. Schreurs, A. Caddemi, and V. Marković, "Artificial neural network based modeling of FinFET forward transmission coefficient," *in Proc. 10th International Conference on Telecommunications in Modern Broadcasting, Cable and Satellite Communications – TELSIKS 2011,* vol. 1, Niš, Serbia, Oct. 2011, pp. 238-241.